Paleobiology and comparative morphology of a late Neandertal sample from El Sidrón, Asturias, Spain

Antonio Rosas[a,b], Cayetana Martínez-Maza[a], Markus Bastir[a,c], Antonio García-Tabernero[a], Carles Lalueza-Fox[d], Rosa Huguet[e], José Eugenio Ortiz[f], Ramón Julià[g], Vicente Soler[h], Trinidad de Torres[f], Enrique Martínez[i], Juan Carlos Cañaveras[j], Sergio Sánchez-Moral[k], Soledad Cuezva[k], Javier Lario[l], David Santamaría[m], Marco de la Rasilla[m], and Javier Fortea[m]

[a]Departamento de Paleobiología, Museo Nacional de Ciencias Naturales, Consejo Superior de Investigaciones Cientificas (CSIC), Calle José Gutierrez Abascal 2, 28006 Madrid, Spain; [d]Departament de Biologia Animal, Facultat de Biologia, Universitat de Barcelona, Avenida Diagonal 645, 08028 Barcelona, Spain; [e]Área de Prehistoria, Universitat Rovira i Virgili, Plaça Imperial Tarraco 1, 43005 Tarragona, Spain; [f]Escuela Técnica Superior de Ingenieros de Minas, Universidad Politécnica de Madrid, Calle Ríos Rosas 21, 28003 Madrid, Spain; [g]Instituto Jaume Almera, CSIC, Calle Lluís Solé i Sabarís s/n, 08028 Barcelona, Spain; [h]Instituto de Productos Naturales, CSIC, Avenida Astrofísico Francisco Sánchez 3, 38206 Santa Cruz de Tenerife, Spain; [i]Departamento de Geología, Universidad de Oviedo, Calle Jesús Arias de Velasco s/n, 33005 Oviedo, Spain; [j]Departamento de Ciencias de la Tierra, Universidad de Alicante, Apartado de Correos 99, 03080 Alicante, Spain; [k]Departamento de Geología, Museo Nacional de Ciencias Naturales, CSIC, Calle José Gutierrez Abascal 2, 28006 Madrid, Spain; [m]Departamento de Historia, Universidad de Oviedo, Calle Teniente Alfonso Martínez s/n, 33011 Oviedo, Spain; [c]Hull–York Medical School, University of York, Heslington, YO 105DD, England; and [l]Departamento de Ciencias Analíticas, Universidad Nacional de Educación Distancia, Paseo Senda del Rey 9, 28040 Madrid, Spain

Fossil evidence from the Iberian Peninsula is essential for understanding Neandertal evolution and history. Since 2000, a new sample ≈43,000 years old has been systematically recovered at the El Sidrón cave site (Asturias, Spain). Human remains almost exclusively compose the bone assemblage. All of the skeletal parts are preserved, and there is a moderate occurrence of Middle Paleolithic stone tools. A minimum number of eight individuals are represented, and ancient mtDNA has been extracted from dental and osteological remains. Paleobiology of the El Sidrón archaic humans fits the pattern found in other Neandertal samples: a high incidence of dental hypoplasia and interproximal grooves, yet no traumatic lesions are present. Moreover, unambiguous evidence of human-induced modifications has been found on the human remains. Morphologically, the El Sidrón humans show a large number of Neandertal lineage-derived features even though certain traits place the sample at the limits of Neandertal variation. Integrating the El Sidrón human mandibles into the larger Neandertal sample reveals a north–south geographic patterning, with southern Neandertals showing broader faces with increased lower facial heights. The large El Sidrón sample therefore augments the European evolutionary lineage fossil record and supports eco-geographical variability across Neandertal populations.

Neandertal morphology evolved in the northwestern corner of the Old World through a long evolutionary process, whose fossil evidence is present through the European Middle and Late Pleistocene geological record (1–6). In this process, variation across the geographical range of Neandertals through its evolutionary history should be evident. The recovery of mtDNA in an increasingly number of early Late Pleistocene specimens is beginning to document an emerging Neandertal phylogeographic pattern (7–9), and this pattern may be present as well in their skeletal morphology.

The paleoanthropological collection presently retrieved at the El Sidrón cave site (Asturias, Spain) represents the most significant Neandertal sample in the Iberian Peninsula, and it allows further insight into these evolutionary processes and diversification of Middle Paleolithic populations across geographic regions. At a local scale, the El Sidrón site fulfills a significant gap in the fossil record of the Cantabrian region. A long tradition of Paleolithic research in the region (10) has yielded a rich Pleistocene cultural record (e.g., El Castillo, La Viña, El Pendo, Morín), but the scarcity of human remains has precluded a characterization of the humans inhabiting the area. The large sample from El Sidrón provides a portrait of those late Neandertals living in the Cantabrian range.

El Sidrón Site

The accidental unearthing in 1994 of an outstanding set of human fossils gave rise to the archeological excavation and multidisciplinary study of the site (11). As a result, a significant archeopaleontological record is being recovered, largely composed of Neandertal remains. The karstic site of El Sidrón is located in the region of Asturias, Spain, (43°23′01″N, 5°19′44″W) (Fig. 1). Geologically, the site is found in the so-called "Surco Oviedo-Infiesto" (11), a strip of Mesozoic and Cenozoic sediments limited by Paleozoic relief to the north and south. The cavity is a pression tube of ≈600 m long, with a central stretch of 200 m oriented nearly west–east ("Galería del Río"). This tube shows on its southern bank transverse galleries in a NE–SW to N–S direction, generally of a restricted nature. The fossil site is located in one of these transverse galleries, the Osario Gallery, of ≈28 m long and 12 m at its widest part (Fig. 1). All of the remains are recovered from a surface ≤6 m^2 within stratum III of the sedimentary sequence. Sediments accumulated in the Osario Gallery constitute a relatively thin deposit, so far prospected at a maximum thickness of 227 cm.

The archeological assemblage recovered at the site is in secondary position, and it certainly comes from a close exterior location. *Ex hypothesis*, the original deposit was located outside the cavity, possibly in a doline close to the vertical of the site. A collapse of nearby fissures produced the sudden entry of the archeological material in a single event. Several taphonomic signals help to clarify the scenario. Refitting of several bone fragments and 53 stone tools indicates a limited displacement as well as synchrony of the assemblage. Preservation of osteological surfaces is excellent with very limited trampling and erosion. There are no toothmarks of large carnivores on the bones, with marginal action of rodents and a small carnivore (e.g., fox) on a few nonhuman remains. A few bones

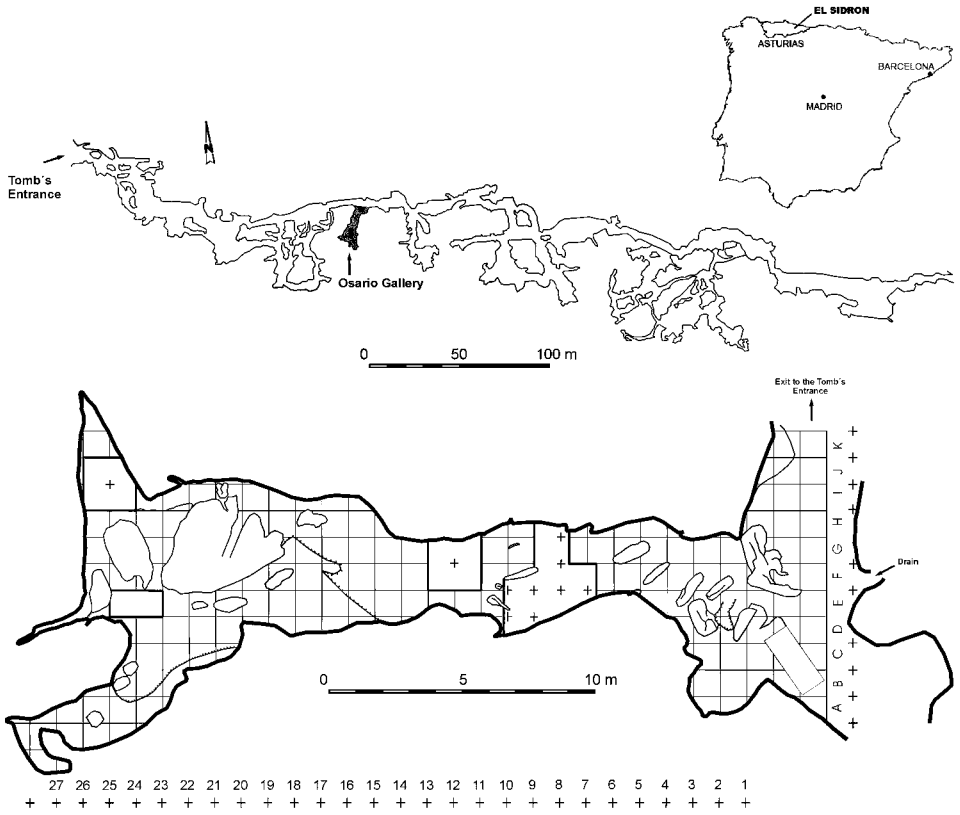

Fig. 1. Localization of the El Sidrón site in Asturias (Spain). A map of the cave system with the Osario Gallery show the excavated area.

have hydraulic abrasion but no weathering. In short, the data point to a limited exposure of bones outside the cavity; a mass displacement moved the archeological deposit into the cave secondarily, with very little movement after final deposition.

Dating. Three human specimens were ^{14}C accelerator mass spectrometer-dated: SD-500 (tooth), 40,840 ± 1,200 ^{14}C B.P. (Beta 192065); SD-599a (bone), 37,300 ± 830 ^{14}C B.P. (Beta 192066); and SD-763a (tooth), 38,240 ± 890 ^{14}C B.P. (Beta 192067). Calibrated with CalPal (www.calpal.de), the dates become 44,310 ± 978, 42,320 ± 367, and 42,757 ± 464 cal B.P., respectively, the average calibrated age being 43,129 ± 129 cal B.P. (7). A similar age was obtained from preliminary of amino acid razemization (11), both from gastropods (39,000 ± 7,000) and human fossils 32,000 ± 11,000).

Paleontological Sample. A series of ≈1,323 human remains has been recovered at El Sidrón (Table 1). The collection has been divided into the 140 specimens unprofessionally unearthed (labeled SDR) $(11–14)^n$ and the systematically recovered sample (labeled SD) (11). Refitting of bones and stone tools derived from both sets largely testifies to a single archeological deposit. All of the skeletal parts are represented in the sample, and at least eight individuals have been identified: one infant, one juvenile, two adolescents, and four young adults. Nonhuman bones are very scarce (Table 1), with the presence of *Cervus elaphus*, a large bovid, very few small mammals and gastropods.

Ancient DNA. Mitochondrial DNA (mtDNA) sequences have been retrieved so far from two El Sidrón samples (10): a right I^2 (SD-441) and a femur fragment (SD-1252; SI2 in ref. 9). The first sample yielded a 48-bp sequence (between positions 16,230 and 16,278 of the mtDNA reference sequence), and the second yielded an almost complete mtDNA hypervariable region 1 (302-nt sequence, between positions 16,076 and 16,378). The sequences are identical in the overlapping 48-bp segment, and thus it cannot be discarded from the genetic data that they belong to the same individual.

Lithics. A total of 333 lithic artifacts have been recovered, including side scrapers, denticulates, a hand axe, and several Levallois points. The raw material comes from the immediate cave environment, and it is mostly chert, and quartzite in a lesser proportion. The lithic assemblage is largely flake-based, with a few laminar products and some Levallois supports. Also, up to 17 flakes, some of them retouched, have been refitted on a core fragment, reflecting knapping at the primary location of the assemblage.

Morphological Affinities of the Human Remains

The El Sidrón teeth are large, with crenulated enamel and accessory cusps. Neandertal lineage incisive features (16) observed in the sample include shovel-shaping, marked labial convexity, and strongly developed lingual tubercles. On the premolars (17), an asymmetric lingual contour, strong transverse crests, a metaconid

Table 1. Fossil specimens recovered at El Sidrón site

Anatomical region	No. of specimens
Skull and mandible	97
Teeth	108
Upper limb	257
Lower limb	159
Ribs and vertebra	137
Others and indeterminate	565
Nonhuman	7
Total	1,330

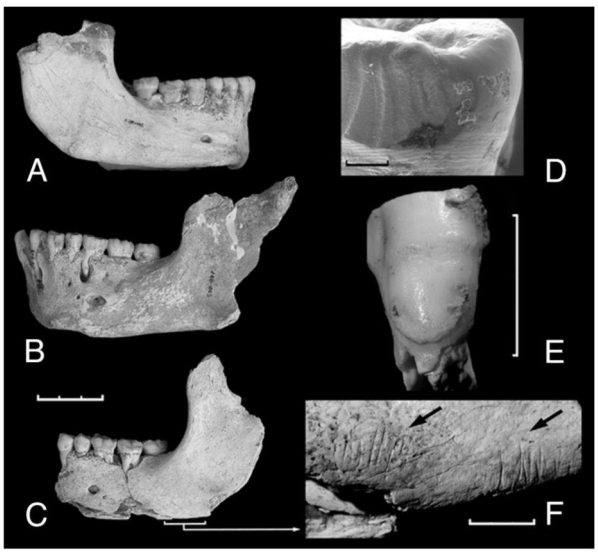

Fig. 2. Mandibles from El Sidrón site and paleobiological aspects of the sample. (*A*) Mandible 1. (*B*) Mandible 2. (*C*) Mandible 3. (*D*) Interproximal facet with subvertical grooves. (*E*), Enamel hypoplasia defects in the specimen SD-1161. (*F*) Cutmarks on the basal border of Mandible 3. [Scale bar: 3 cm (*A–C*); 1 mm (*D*); 1 cm (*E* and *F*).]

lingually located, and accessory lingual cusps are present (e.g., SD-763). The posterior dentition shows some cases of a noticeable taurodontism (e.g., SD-531). No upper face skeletal remains have been recovered, but three mandibles are well preserved (Fig. 2). The mandibular body tends to be high and thick. The mental trigone is strongly developed without any sign of a submental notch. Interestingly, the retromolar space is short in these mandibles. Other characteristic Neandertal lineage features include mental foramen below M_1, deep pterygoid fossa, and inclined mylohoid line.

The neurocranium is well represented in the sample but fragmentary. Overall, the anatomy of these fossils corresponds to the set of features detected in Late Pleistocene Neandertals. The SD-436 frontal preserves a portion of the right squama and part of the supraorbital torus, with the superciliary region preserved. It shows a marked anterior projection with the development of a supraglabellar fossa, and the supratoral sulcus is well defined; there is a rounded torus with apparent lateral continuity among the three elements and a high degree of pneumatization reaching the lateral trigone. SD-438 is an immature right supraorbital torus and a portion of the squama. It shows a marked projection of the supraorbital torus and a clear supratoral sulcus. The temporal bones (SD-315 and SD-359) are still covered by concretions, but several diagnostic features (18) can be distinguished, including a low projection of the mastoid process, flattened glenoid fossa, and an inclined anterior wall of this fossa. Two occipital bones have been recovered. SD-1219 is a reasonably complete occipitomastoid region (Fig. 3), with the upper occipital scale and temporal petrosal in good condition but a badly fragmented basilar part. The occipital is large, with a marked nuchal torus and open sutures connecting with a well preserved temporal pyramid. A large suprainiac fossa is present (Fig. 3). SD-1149 is smaller and partially covered by thin breccia. Right transverse sinuses are observed in both cases.

The postcranial skeleton is principally represented by hand and foot metapodials and phalanges, the latter being the most abundant bones in the assemblage (Table 1). Size and robustness of the first metacarpal and the enlarged distal tuberosity in the distal hand phalanges are among the diagnostic features. Included in a block (SD-437) are several bones of an adult foot in anatomical connection. Humeri (one complete), as well as fibulae and radii are also represented in the sample. The lower limb is poorly preserved, with an immature coxal fragment and remains of femora and tibiae, with thick cortical bone.

Paleobiological Aspects of El Sidrón Human Remains

Paleobiology of El Sidrón sample shares, in several aspects, the common pattern for Neandertal populations: high incidence of dental hypoplasia and interproximal grooves, although no serious traumatic lesions are present (19). There are no "toothpick" grooves (20–22) so far in the El Sidrón dental sample. Adult 4 shows an elongated nonmasticatory wear in the mesial side of left lower canine, denoting the use of the mouth in activities other than mastication.

Dental Hypoplasia. Neandertals have been noted to have high levels of developmental stress indicators, especially dental enamel hypoplasias, indicating growth arrest periods (23–26). All of the individuals from El Sidrón present dental hypoplasia. Defects are well marked on the incisors (59%), canines (50%), premolars (58%), and molars (32%). Five individuals present two events of arrest, whereas Adult 3 shows up to four. Adolescent 2 presents an exceptionally severe episode of physiological stress. The highest frequency of hypoplasia is found to occur near the 4th year of life. Besides, four individuals also present dental hypoplasia near the 12th year of life. These data suggest weaning and adolescence as the life-history events more prone to nutritional stress (23) in the El Sidrón sample as well as significant survival of such events.

Paleopathology. Dental calculus is present, at variable degrees, in the adults and the adolescents. Mandible 2 shows alveolar bone resorption and an apical abscess (Fig. 2), consistent with a chronic apical peridontitis associated with traumatic occlusion (27). This sort of lesion is common among Neandertal lineage populations (28).

Interproximal Tooth Wear. Tooth-to-tooth contact occasionally shows a number of subvertical grooves, frequently found in

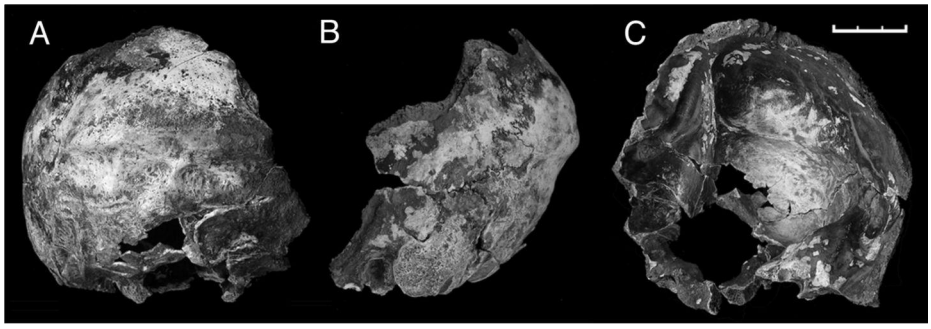

Fig. 3. SD-1219 El Sidrón occipitomastoid region. Shown are posterior (*A*), left side (*B*), and interior (*C*) views. (Scale bar: 3 cm.)

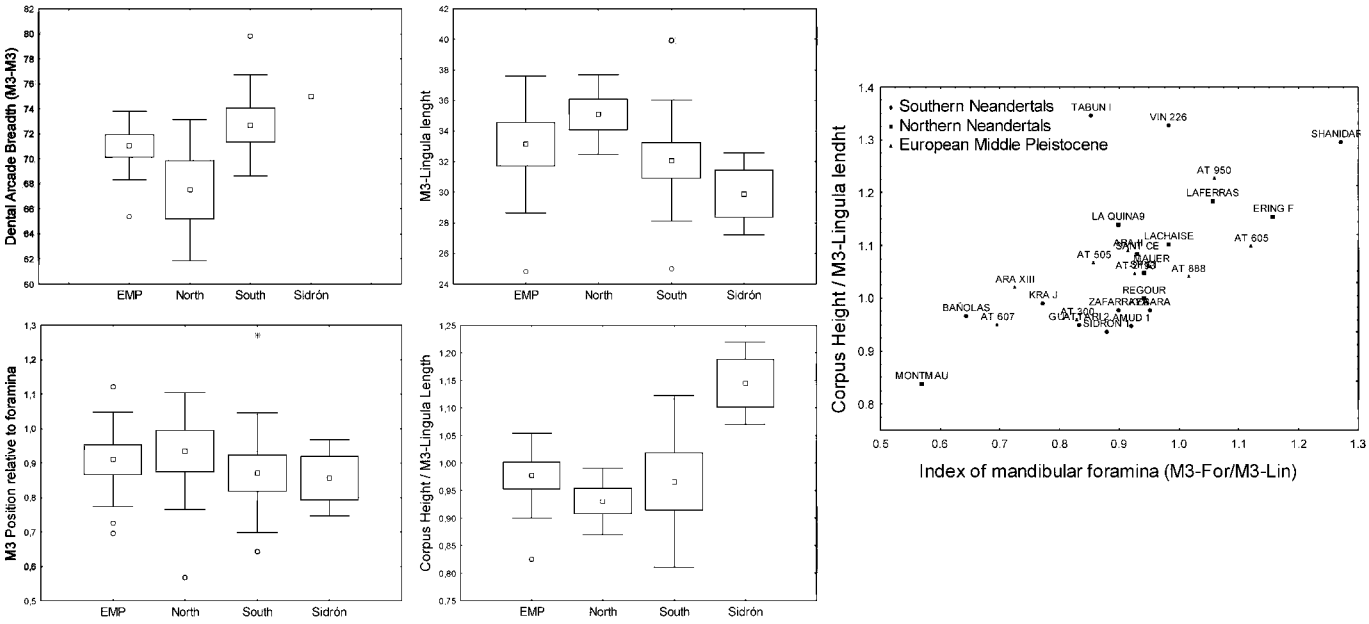

Fig. 4. Mandibular measurements and indices suggesting geographic patterning in Neandertal populations. (*Left* and *Center*) Box plots of significantly different variables in a north–south geographic polarity. Box plots provide means, mean ± SE (box), and mean ± SD (whiskers). (*Right*) Outliers appear as circles. Scatter plot of two indices of mandibular variables is shown. EMP, European Middle Pleistocene; Northern, northern Neandertals; Southern, southern Neandertals; For, mental foramen; M3, bucodistal corner of the alveolus; Lin, Lingula mandibulae. Corpus height is at the level of the mental foramen. EMP specimens were from Arago, Mauer, and Atapuerca-SH. Northern Neandertals were from La Ferrassie, La Quina, Le Moustier, La Chapelle-aux-Saints, St. Césaire, La Chaise (L' Abri Suard), Spy, Regourdou, Ehringsdorf, and Aubesier. Southern Neandertals were from El Sidrón, Guattari, Zafarraya, Krapina, Vindija, Amud, Kebara, Tabun, and Shanidar.

Neandertal teeth (29, 30) and occasionally in other humans (31, 32). El Sidrón adults and adolescents all show interproximal grooves in 11 incisors, 5 canines, 17 premolars and 19 molars, ranging from 1 to 8 grooves per tooth (Fig. 3). The proximate causes of subvertical grooves have been controversial (29, 32), but it is generally accepted that they derive from high levels of masticatory stress, congruent with other aspects of Neandertal dental apparatus: beveling, labial wear striae, and nonocclusal wear (29, 33), attributes also observable in the El Sidrón sample.

Human-Induced Bone Modification. Unequivocal evidence of human-induced modification of human bones is observed in the Neandertals from El Sidrón. Methodology and quantification follow the criteria in ref. 34. Anthropic activity is evinced by the presence of cut marks, flakes, percussion pitting, conchoidal scars, and adhering flakes. Immature skull bones (frontal, temporal, and parietal) show a higher frequency of cut marks, possibly indicating skinning activities. Long bones (humerus, ulna, radius, and tibia) show short and deep cut marks related to disarticulation processes.

In contrast to other sites (35, 36), individuals seem to have been treated differentially. For instance, Mandible 3 shows clear cut marks on the ramus basal border (Fig. 3), whereas the others do not display any evidence of defleshing. It is generally accepted that the inference of cannibalism must be supported by a similarity of the modifications on the human remains to modifications of nonhuman remains (35, 36). The scarcity of faunal remains in the El Sidrón sample prevents a direct comparison with human bones. Yet, the clear evidence of bone breaking (conchoidal percussion scars) is presumably related to processing for marrow and brains, which strongly suggest a nutritional exploitation. Given the high level of developmental stress in the sample, some level of survival cannibalism would be reasonable.

El Sidrón Human Remains and Neandertal Geographic Variation

The evolutionary place of El Sidrón Neandertals has been investigated in the context of possible Neandertal geographic patterning. The mandible, as an anatomical system with clear European lineage-derived features, has been largely used, maximizing the intra-El Sidrón variability ($n = 3$). The comparative samples were divided into regional subgroups according to north–south and east–west geographic polarities. Specimens coming from the southwest Asia and south European peninsulas (Iberian, Italian, and Balkans) are included in the southern subset. The east–west boundary is established by the Adriatic Sea, with the Balkans in the east.

Pairwise t test comparisons did not show differences between east and west. By contrast, a number of variables showed significant differences in a north–south division (Fig. 4). The position of the M_3 in relation to other mandibular structures emerges as a determinant for the differences. Bi-M_3 arcade width ($t = 2{,}2711$; df $=14$; $P < 0.03$) and M_3–lingula length ($t = -2{,}1964$; df $= 19$; $P < 0.04$) show significant differences in a north–south polarity. Appreciable differences also hold for a variety of indices relating the latter variables with the M_3–mental foramen length and corpus height (Fig. 4) (e.g., M_3–lingula/M_3–mental foramen, t test nonsignificant). Southern mandibles are wider at the level of the M_3 and the coronoid process, and the corpus is located relatively closer to the ramus (e.g., shorter retromolar spaces). By contrast, northern mandibles are narrower, and the corpus–ramus distance is larger. This geographic patterning signal was further tested by geometric morphometrics.

The partial least-squares analysis allows visualization of the differences (Fig. 5*A*). The morphological pattern associated with northern Neandertal populations shows relatively higher prognathism (longer corpus). In addition, the southern populations are characterized by a relatively shorter corpus (reduced retromolar space) and vertically high posterior faces (see also Fig. 3). The height of the mandible, as recorded by linear measurements, is reflected by the height of the corpus as well as of the ramus. Overall, the geographic variation is not related to variation in overall mandibular size (centroid size is not statistically significantly different between northern and southern subsamples).

Procrustes distance of the three-dimensional (3D) data between northern and southern populations of Neandertals is $d =$

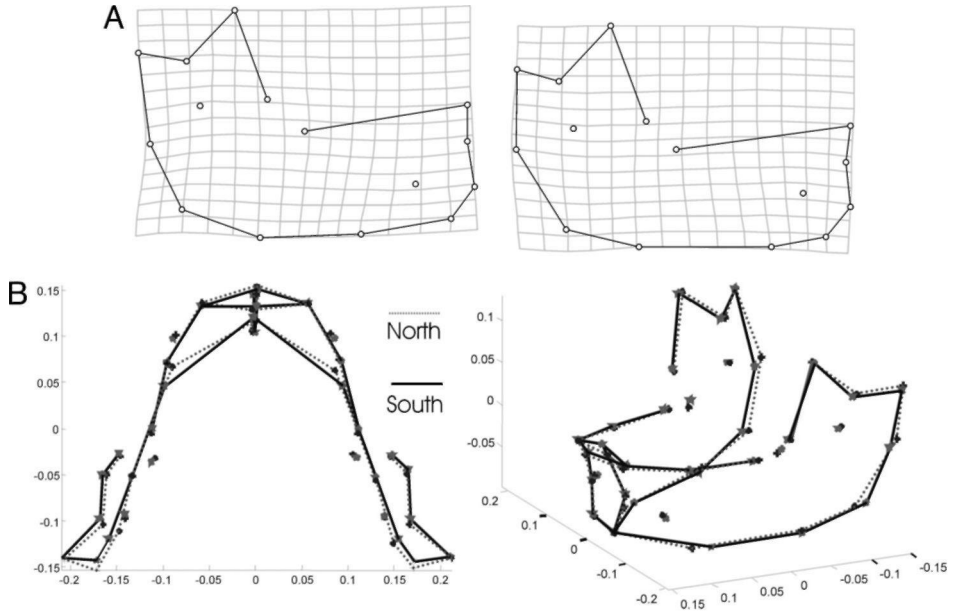

Fig. 5. Thin-plate spline transformations of the mean shape into a predicted shape according to singular vector scores of a north–south axis. (*A*) Partial least-squares analysis. (*B*) 3D mean shape differences between northern and southern Neandertal samples.

0.049, and it is statistically highly significant ($F = 1.4565$; df1 = 95; df2 = 1,615; $P < 0.003$) (Fig. 5*B*). Simultaneously, mean shape differences between Neandertals and the EMP group were highly statistically significant. Interestingly, 3D procrustes distances between the EMP sample and those of southern and northern Neandertal subsamples show closer morphological affinities of the EMP to the northern subsample (EMP–northern Neandertals: $d = 0.048$; $F = 1.84$; df1 = 95; df2 = 1,615; $P < 0.001$; EMP–southern Neandertals: $d = 0.044$; $F = 1.6949$; df1 = 95; df2 = 1,805; $P < 0.001$). The permutation analyses support these findings. In all comparisons the 99th percentile of the F distribution was clearly below the observed F score (within Neandertals observed $F = 1.4565$, 99th percentile of permuted $F = 1.37$; between EMP and northern Neandertals: observed $F = 1.8489$, 99th percentile of permuted $F = 1.7$; and between EMP and southern Neandertals: observed $F = 1.6949$, 99th percentile of permuted $F = 1.5763$).

Discussion

Presently, most of the scholars agree that Neandertals constitute a distinct human evolutionary lineage not involved in the initial ancestry of modern humans. The causes promoting the Neandertal anatomical pattern, nevertheless, are still under debate (37–39). Climatic adaptation is a major factor invoked to accounting for most of the Neandertal anatomy (40, 41), although biomechanical adaptations (42, 43) and stochastic genetic processes (44) are raised for the explanation of specific traits. Clarification of these aspects has focused the research interest on the evolution of this archaic human group, and the amount of interbreeding between Neandertals and early modern humans after the arrival of the latter to Europe is a matter of contention (45–47).

Given the establishment of a Neandertal evolutionary lineage in Europe, we are beginning to address issues regarding the population history of Neandertals *sensu stricto*. Genealogical analyses of the ancient mtDNA sequences are showing well defined genetic groups, suggesting the existence of different lineages within the Neandertal gene pool (8, 9). In the context of Quaternary ecoclimatic instability, the evolution of Neandertals has been long enough to produce regional diversity of populations. If Middle Paleolithic human populations behaved as part of the Paleartic bioma, it would not be surprising if they exhibited the marked north–south faunal provinciality detected in Europe at least during the OIS 3 (48).

Morphometric Implications. The analysis of mandibular variability conforms to a pattern of geographic distribution in a north–south polarity within Neandertal samples, in which southern populations may have developed a slightly distinctive craniofacial pattern. This conclusion may find support in recent research (49), showing that mandibular morphology records geographic patterning in modern humans.

Two sets of traits seem to be involved in the north–south differences. On the one hand, there is the breadth of the mandible, indicated by classic distances (e.g., Bi–M_3 breadth), 3D procrustes distances, and the variation in discrete features, especially in the eversion of gonion. On the other hand, there is the relative position of the ramus with respect to the corpus (e.g., M_3–lingula length). The latter is associated with the retromolar space size, irrespective of the ramus breadth. Retromolar spaces are moderately developed in the El Sidrón, despite the large size of the mandibles, even though this feature is partially determined by allometry in Neandertals and other species (49, 50). Metrics and discrete features point to a reduced midfacial prognathism in the El Sidrón individuals, and the same have been noted in other Iberian Neandertals (e.g., Valdegoba) (51). Therefore, southern Neandertals seem to present broader and shorter faces, with the architecture of the middle face (broader zygomatic arches with gonion eversion) directly involved in this pattern.

Neandertal populations were largely isolated by geographic barriers (52–55), and at the peak of glacial events the European population was mainly concentrated in the south of the continent (54). In this framework, two properties should be expected for the southern populations. First, they should have had a larger temporal continuity, and in consequence more time for developing morphological variants. Second, a larger amount of variability should be found in these populations. The first expectation may be substantiated by the fact that northern samples are morphologically more similar to those from the Middle Pleistocene; that is, Neandertal populations from the north would maintain a more primitive condition within the European lineage. If so, the slightly distinctive morphology of southern samples may be interpreted as derived. Yet, southern samples (e.g., Krapina, El Sidrón) illustrate local variation that might be explored from this perspective.

Summary. The Iberian Neandertal sample from El Sidrón substantially improves the fossil record of these humans, allowing new explorations into the geographic context of Neandertal evolution.

The analysis of mandibular variability supports the hypothesis for the identification of northern and southern varieties of Neandertals, in which southern populations may have developed a slightly reduced midfacial prognathism. At the same time, the paleobiology and human-induced modifications of the eight individuals identified in the El Sidrón sample fit well with the established Neandertal patterns. The El Sidrón sample is therefore both expanding our knowledge of Neandertals in Iberia and modifying our perceptions of Neandertal population biology and evolution.

Materials and Methods

Comparative samples comprise 32 Neandertal and 23 European Middle Pleistocene mandibles. Thirty-seven linear distances (56, 57) as well as 2D (58–60) and 3D landmark coordinates were obtained from original fossils or good quality casts. Landmarks were digitized by using a MicroScribe 3DX digitizer (Immersion Corp., San Jose, CA) (58).

2D Geometric Morphometrics. A partial least-squares analysis was performed using the 2D data of 19 mandibles (59, 60). Partial least-squares analysis helped to find correlated pairs of linear combinations (singular vectors) between two blocks of variables (61, 62). Detailed technical information about the method in geometric morphometrics is relatively new (63, 64). The singular vectors are constructed in the form of new, paired "latent" variables (one per block, also called "singular warps") (64) that account for as much as possible of the covariation between the two original sets of variables. In a sense similar to a principal-components analysis (PCA), the singular-value decomposition (SVD) describes the data in terms of scores of each specimen along singular axes, singular values (similar to eigenvalues), and loadings (singular vectors, similar to eigenvectors). However, singular-value decomposition is applied with a different goal, i.e., to maximize low-dimensional representation of between-block covariance (SVD) vs. maximizing low-dimensional representation of total sample covariance (PCA). The singular warps display the maximal covariance between both the shape variables within-block (mandibles) and with the variables of the other block (geographic distribution) (61, 62, 64). The associated morphological patterns are visualized by singular warps (64), which are thin-plate spline transformations of the mean shape into a predicted shape according to singular vector scores of the given axis (north–south).

3D Geometric Morphometrics. Further the hypotheses of geographic differences within northern and southern Neandertals and that of species specific shape differences between those and EMP humans were tested by Goodall's F tests (65) (34 3D landmarks). This test is based on mean shape comparisons. It compares the deviation of squared Procrustes distances in shape space from the group means and compares them with the variance around the grand mean and assesses the ratio of explained and unexplained variances of group factors (65). This test was accompanied by a permutation test (n = 2500), which permutes specimens of groups at random and calculates the F distribution of random group comparisons against which the observed F score can be compared. These analyses give a further estimate of the significance of Goodall's F test, and they were performed by using Simple3D-IMP software (Integrated Morphometrics Package) (15, 66).

We thank A. Estalrrich, S. García, A. Cruz, and M. Pérez for help managing the fossil collection; all of the people working at the El Sidrón excavation for their effort and interest; and E. Trinkaus for improving the quality of the text and providing 3D data from some significant specimens. This work was supported by Principado de Asturias-Universidad de Oviedo Grant CN-04-152. Partial aspects of the investigation are included in Project BOS2003–01531, Spanish Ministerio de Educación y Ciencia.

1. Howell FC (1960) *Curr Anthropol* 1:195–228.
2. Bermúdez de Castro JM (1986) *J Hum Evol* 15:265–287.
3. Rosas A, Bermúdez de Castro JM (1998) *Geobios* 31:687–697.
4. Trinkaus E (1988) in *L'Homme de Neandertal, l'Anatomie 3*, ed Trinkaus E (ERAUL 30, Liège), pp 11–29.
5. Hublin JJ (1988) in *L'Homme de Neandertal, l'Anatomie 3*, ed Trinkaus E (ERAUL 30, Liège), pp 81–94.
6. Arsuaga JL, Martínez I, Gracia A, Lorenzo C (1997) *J Hum Evol* 33:219–281.
7. Lalueza-Fox C, Sampietro ML, Caramelli D, Puder Y, Lari M, Calafell F, Martinez-Maza C, Bastir M, Fortea J, de la Rasilla M, *et al.* (2005) *Mol Biol Evol* 22, 1077–1081.
8. Caramelli D, Lalueza-Fox C, Condemi S, Longo L, Milani L, Manfredini A, de Saint Pierre M, Adoni F, Lari M, Giunti P, *et al.* (2006) *Curr Biol* 16:630–631.
9. Lalueza-Fox C, Krause J, Caramelli D, Catalano G, Milani L, Sampietro ML, Calafell F, Martínez-Maza C, Bastir M, García-Tabernero A, *et al.* (2006) *Curr Biol* 16:629–630.
10. Freeman LG (2005) in *Neandertales Cantábricos, Estado de la Cuestión*, eds Montes R, Lasheras JA (Monografias 20, Museo de Altamira, Cantabria), pp 21–38.
11. Fortea J, de la Rasilla M, Martínez E, Sánchez-Moral S, Cañaveras JC, Cuezva S, Rosas A, Soler V, Juliá R, Torres T, *et al.* (2003) *Estud Geol* 59:159–180.
12. Rosas A, Aguirre E (1999) *Estud Geol* 55:181–190.
13. Egocheaga JE, Trabazo R, Rodríguez L, Cabo LL, Sierra MJ (2000) *Bol Cien Nat Real Ins Estud Astur* 46:219–263.
14. Prieto JL, Abenea J, Montes R, Sanguino J, Muñoz E (2001) *Munibe* 53:19–29.
15. Sheets HD (2001) *IMP, Integrated Morphometric Package* (www.canisius.edu/~sheets/morphsoft.html).
16. Bermúdez de Castro JM (1988) *J Hum Evol* 17:279–304.
17. Bailey SE, Lynch JM (2005) *Am J Phys Anthropol* 126:268–277.
18. Martínez I, Arsuaga JL (1997) *J Hum Evol* 33:283–318.
19. Berger TD, Trinkaus E (1995) *J Archaeol Sci* 22:841–852.
20. Ungar PS, Grine FE, Teaford MF, Pérez-Pérez A (2001) *Arch Oral Biol* 46:285–292.
21. Lebel S, Trinkaus E (2002) *J Hum Evol* 43:659–685.
22. Trinkaus E, Marks AE, Brugal J-P, Bailey SE, Rink WJ, Richter D (2003) *J Hum Evol* 45:219–226.
23. Ogilvie MD, Curran BK, Trinkaus E (1989) *Am J Phys Anthropol* 79:25–41.
24. Bermúdez de Castro JM, Pérez PJ (1995) *Am J Phys Anthropol* 96:301–314.
25. Cunha E, Ramírez Rozzi F, Bermúdez de Castro JM, Martinón-Torres M, Wasterlain SN, Sarmiento S (2004) *Am J Phys Anthropol* 125:220–231.
26. Guatelli-Steinberg D, Larsen CS, Hutchinson DH (2004) *J Hum Evol* 47:65–84.
27. Prieto JL (2005) in *Neandertales Cantábricos, Estado de la Cuestión*, eds Montes R, Lasheras JA (Monografias 20, Museo de Altamira, Cantabria), pp 397–343.
28. Lebel S, Trinkaus E, Faure M, Fernandez P, Guérin C, Ritcher, D., Mercier N, Valladas H, Wagner G (2001) *Proc Natl Acad Sc USA* 98:11097–11102.
29. Villa G, Giacobini G (1995) *Am J Phys Anthropol* 96:51–62.
30. Egocheaga JE, Pérez-Pérez A, Rodríguez L, Galbana J, Martínez LM, Antunes MT (2004) *Anthropologie* 42:49–52.
31. Pérez-Pérez A, Espruz V, Bermúdez de Castro JM, de Lumley MA, Turbón D (2003) *J Hum Evol* 44:497–513.
32. Kaidonis JA, Towsend GC, Richards LC (1992) *Am J Phys Anthropol* 88:105–107.
33. Ungar PS, Fennell KJ, Gordon K, Trinkaus E (1997) *J Hum Evol* 32:407–421.
34. Fernández-Jalvo Y, Díez J C, Cáceres I, Rosell J (1999) *J Hum Evol* 37:591–622.
35. White TD (1992) *Prehistoric Cannibalism at Mancos 5MTUMR* 2346 (Princeton Univ Press, Princeton).
36. Defleur A, White T, Valensi P, Slimak L, Crégut-Bonnoure E (1999) *Science* 286:128–131.
37. Antón SC (1994) in *Integrative Paths to the Past: Paleoanthropological Advances in Honor of F. Clark Howell*, ed Ciochon R (Prentice–Hall, Englewood Cliffs, NJ), pp 677–695.
38. Churchill SE (1998) *Evol Anthropol* 46:46–60.
39. Franciscus RG (2003) *J Hum Evol* 44:701–729.
40. Trinkaus E (1981) in *Aspects of Human Evolution*, ed Stringer CB (Taylor & Francis, London), pp 187–224.
41. Holliday TW (1997) *Am J Phys Anthropol* 104:245–258.
42. Rak Y (1986) *J Hum Evol* 15:151–164.
43. Spencer MA, Demes B (1993) *Am J Phys Anthropol* 91:1–20.
44. Dean D, Hublin JJ, Holloway R, Ziegler R (1998) *J Hum Evol* 4:85–508.
45. Trinkaus E (2005) *Annu Rev Anthropol* 34:207–230.
46. Tattersall I, Schwartz JH (1999) *Proc Natl Acad Sci USA* 96:7117–7119.
47. Klein RG (2003) *Science* 299:1525–1527.
48. Stewart JR (2005) *Quaternary Int* 137:35–46.
49. Nicholson E, Harvati K (2006) *Am J Phys Anthropol* 131:368–383.
50. Rosas A, Bastir M (2004) *Anat Rec A* 278A:551–560.
51. Quam RM, Arsuaga JL, Bermúdez de Castro JM, Díez CJ, Lorenzo C, Carretero M, García N, Ortega AI (2001) *J Hum Evol* 41:385–435.
52. Hewitt G (2000) *Nature* 405:907–913.
53. Howell FC (1952) *Southw J Anthropol* 8:377–410.
54. Hublin JJ (1998) in *Neandertals and Modern Humans in Western Asia*, eds Akazawa T, Aoki K, Bar-Yosef O (Plenum, New York), pp 295–310.
55. Howell FC (1957) *Q Rev Biol* 32:330–347.
56. Rosas A (1995) *J Hum Evol* 28:533–559.
57. Rosas A (1997) *J Hum Evol* 33:319–331.
58. Rosas A, Bastir M (2002) *Am J Phys Anthropol* 117:236–245.
59. Bastir M, Rosas A (2005) *Am J Phys Anthropol* 128:26–34.
60. Bastir M, Rosas A, Sheets DH (2005) in *Modern Morphometrics in Physical Anthropology*, ed Slice D (Kluwer, Boston), pp 265–284.
61. Bookstein FL (1991) *Morphometric Tools for Landmark Data* (Cambridge Univ Press, Cambridge, MA).
62. Rohlf FJ, Corti M (2000) *Systematic Zool* 49:740–753.
63. Zelditch ML, Swiderski DL, Sheets HD, Fink WL (2004) *Geometric Morphometrics for Biologists: A Primer* (Elsevier, San Diego).
64. Bookstein FL, Gunz P, Mitteroecker P, Prossinger H, Schaefer K, Seidler H (2003) *J Hum Evol* 44:167–187.
65. Goodall C (1991) *J R Stat Soc B* 53:285–339.